

Unitarity effects in like-charge W pair production

A. Abbasabadi

Physical Sciences Department, Ferris State University, Big Rapids, Michigan 49307

Wayne W. Repko

Department of Physics and Astronomy, Michigan State University, East Lansing, Michigan 48824

(Received 21 August 1992)

Using the effective- W approximation, we calculate the invariant-mass distribution for the production of W^+W^+ (W^-W^-) via W^+W^+ (W^-W^-) fusion at a pp collider with an energy of 40 TeV. These results are compared with the corresponding results for the production of W^+W^- via W^+W^- fusion. All W polarizations are taken into account. We also study the effects of the unitarity in the W^+W^+ (W^-W^-) scattering, with particular attention to the possibility that the signal for longitudinally polarized W 's will be enhanced when the Higgs sector is strongly interacting.

PACS number(s): 13.85.Qk, 14.80.Er, 14.80.Gt

I. INTRODUCTION

In the standard model of electroweak interaction, the Higgs-boson mass is essentially a free parameter. At the present, there is an experimental lower limit of 48 GeV [1], and some theoretical upper limits of about 1 TeV [2]. Experimental signatures of the Higgs boson are sensitive to its dominant decay mode in a particular mass range. For Higgs-boson mass larger than twice the Z -boson mass, the dominant Higgs-boson decay mode is into gauge-boson pairs W^+W^- and Z^0Z^0 .

As has been noted numerous times, the W^+W^- and Z^0Z^0 pair production processes are excellent probes of the Higgs sector of the standard model [3]. However, these processes are accompanied by relatively large quark-antiquark annihilation and gluon-gluon fusion backgrounds. For the W^+W^+ (W^-W^-) production [4–9], these large backgrounds are absent, although one needs to consider other smaller backgrounds including gluon-exchange channels [5–9] and top quark-antiquark induced processes [7, 9].

There is, however, another feature of W^+W^+ scattering which further complicates its use as a probe of the symmetry-breaking mechanism of the standard model. Recall that it is the scattering of longitudinally polarized W 's and Z 's which provides information about the strength of the symmetry breaking. The couplings of these degrees of freedom are enhanced by a factor m_H/m_W compared to the gauge coupling g , which is characteristic of transversely polarized W 's and Z 's. In the case of W^+W^- scattering, the bulk of the cross section lies in the Higgs peak, and W pairs with an invariant mass in the vicinity of m_H are almost exclusively longitudinally polarized [10]. This makes it possible to explore the symmetry-breaking mechanism near $m_{WW} = m_H$ despite the presence of a large background of transversely polarized W 's from $q\bar{q}$ annihilation. On the other hand, in the standard model, W^+W^+ scattering has no Higgs peak, and the cross section for transversely polarized W 's is much larger than that for longitudinally polarized W 's [7–9] when $0.5 \text{ TeV} \leq m_H \leq 1.0 \text{ TeV}$. It has been shown that additional cuts on the W decays can enhance the

$W_L^+W_L^+$ signal in this region of m_H [7, 9]. Here, in addition to verifying the dominance of transverse polarization in W^+W^+ scattering using the effective- W approximation, we explore the possibility that the longitudinal scattering would dominate in the strongly interacting regime $m_H \gg m_{WW}$.

II. INVARIANT-MASS DISTRIBUTIONS

We use the effective- W approximation [11] to calculate the invariant-mass distribution for the production of W^+ (W^-) pairs. Generally, a rapidity cut η_C of 1.5 is imposed on both final W 's, although less restrictive rapidity cuts are examined. Because the effective- W approximation uses on-shell amplitudes, it is necessary to suppress the Coulomb pole in the t channel due to photon exchange. To accomplish this, we also require a minimum transverse momentum for the both final W 's, $P_T > (P_T)_{\min} = 30 \text{ GeV}$. For $\eta_C = 2.0$, this cut does not affect W^+ (W^-) pairs whose invariant mass m_{WW} exceeds about 650 GeV. In the Higgs-boson propagator, we include a width which is independent of the energy [12], and for quark number structure functions, we use set 2 of the Eichten-Hinchliffe-Lane-Quigg (EHLQ) structure functions [13].

Figure 1 contains all tree-level Feynman diagrams which must be considered in effective- W approximation for the production of the like-charge pairs via gauge-boson fusion. This set of diagrams leads to an amplitude that is gauge invariant and well behaved at large values of m_{WW} the invariant mass of the W^+ (W^-) pairs. In the exact perturbative calculation of $qq \rightarrow qqW^+W^+$, it is necessary to include additional diagrams involving W bremsstrahlung from the quarks [7] in order to maintain gauge invariance.

Our results for like-charge W pair production are summarized in Figs. 2–4. For comparison purposes, we also include the results (in the effective- W approximation) for W^+W^- production via the W^+W^- fusion mechanism [14]. In Figs. 2 and 3, the dominance of the contributions from transversely polarized is clearly illustrated. Figure 2 shows that $W_L^+W_L^+ \rightarrow W_L^+W_L^+$ is only about 10% of the total contribution for a Higgs-boson mass of 0.5 TeV

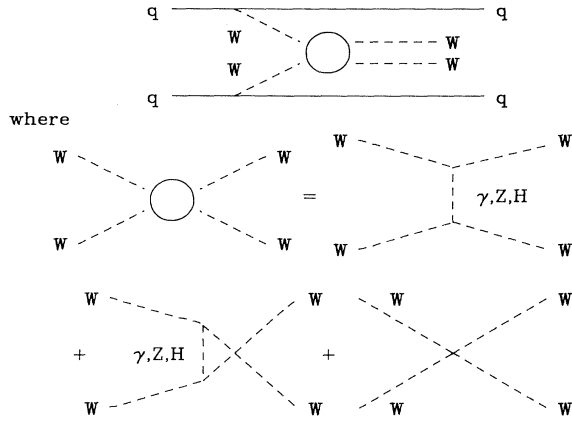


FIG. 1. Feynman graphs for W^+W^+ (W^-W^-) production via W^+W^+ (W^-W^-) fusion.

and $400 \text{ GeV} \leq m_{WW} \leq 1600 \text{ GeV}$. For a Higgs-boson mass of 1 TeV (Fig. 3), the contribution from longitudinal polarizations increases while the transverse contribution remains essentially unchanged. Despite the enhancement of the longitudinal contribution, the transversely polarized W 's still account for the majority of the W^+ pairs. The total cross sections for $m_{WW} \geq 600 \text{ GeV}$ and several rapidity cuts are given in Table I. By imposing a more restrictive cut of $\eta_C = 1$, it is possible to enhance the ratio of longitudinal to transverse pairs, although at the expense of reducing the longitudinal cross section to a relatively small value. We have checked that the longitudinally polarized final state W 's arise almost exclusively from the process $W_L^+W_L^+ \rightarrow W_L^+W_L^+$.

The cross section for the production of W^- pairs is shown in Fig. 4 for a Higgs-boson mass of 1 TeV. Be-

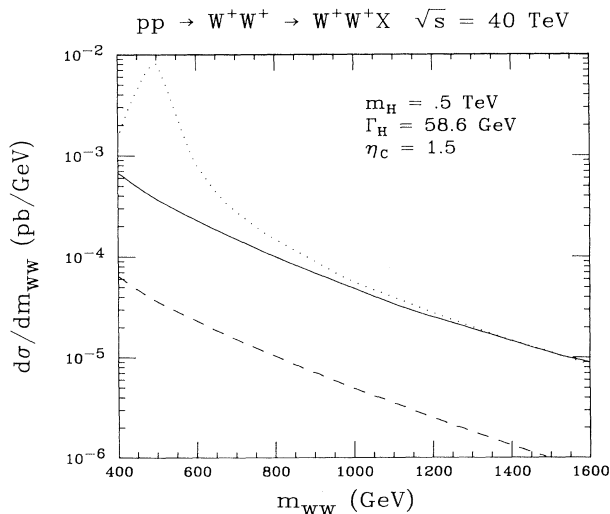


FIG. 2. Invariant-mass distribution for W^+W^+ production in pp collisions at an energy of 40 TeV, with $m_H = 0.5 \text{ TeV}$ and a rapidity cut of 1.5 is shown. The dashed curve is the contribution from initial and final longitudinal W 's, and solid curve is contribution from all polarizations of initial and final W 's. For comparison, the dotted curve is the cross section for the production of W^+W^- pairs via W^+W^- fusion, where all polarizations of initial and final W 's are included.

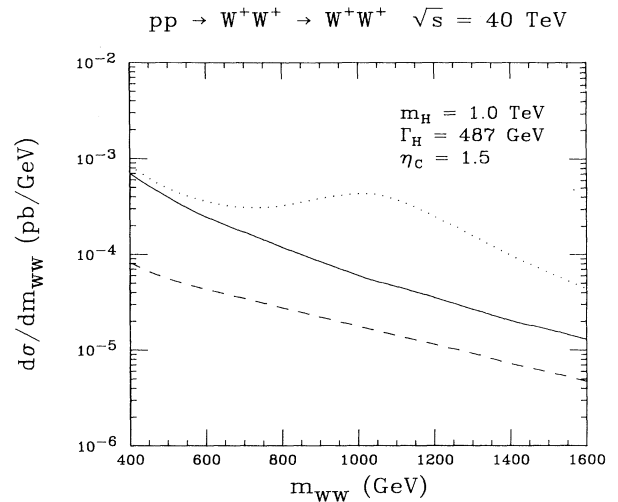


FIG. 3. Same as Fig. 2 with $m_H = 1 \text{ TeV}$.

cause of the lower luminosity in this channel, the total cross section for longitudinally polarized W^- pairs with $m_{WW} \geq 600 \text{ GeV}$ is $\sigma(W_L^-W_L^-) = 7.1 \text{ fb}$ compared to the corresponding $W_L^+W_L^+$ cross section of 17 fb. The W^-W^- cross sections for other polarizations and rapidity cuts are given in parentheses in Table I. In no case does a W^+W^+ cross section exceed the corresponding W^-W^- cross section by more than a factor of 2.5.

In the case of a Higgs-boson mass of 1 TeV and transversely polarized final W^+W^+ , we have compared our result obtained from the effective- W approximation (including the nonleading terms [11, 15]) with the exact perturbative calculation of Barger *et al.* [7]. Although these authors use set 1 of the EHLQ [13] quark number struc-

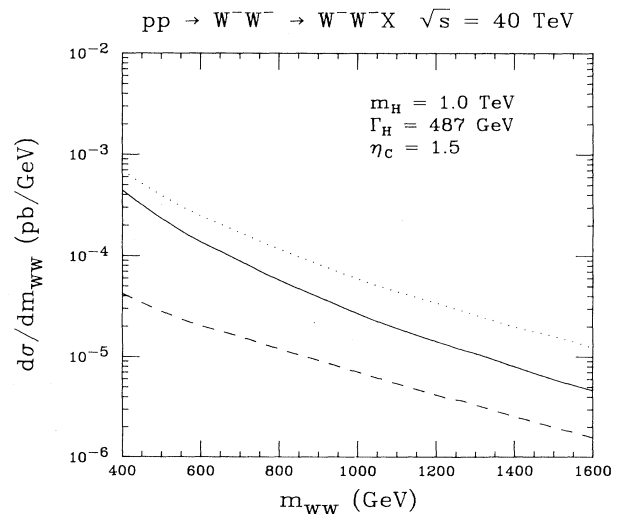


FIG. 4. Invariant-mass distribution for W^-W^- production in pp collisions at an energy of 40 TeV, with $m_H = 1 \text{ TeV}$ and a rapidity cut of 1.5 is shown. The dashed curve is the contribution from initial and final longitudinal W 's, and solid curve is contribution from all polarizations of initial and final W 's. For comparison, the dotted curve is the cross section for the production of W^+ pairs with all polarizations of initial and final W 's are included.

TABLE I. The total cross sections for various polarization states of W^+W^+ (W^-W^-) scattering with $m_{WW} \geq 600$ GeV are given in femtobarns. All calculations are performed using the effective- W approximation for rapidity cuts $\eta_C = 1, 1.5$, and 2. A Higgs-boson mass $m_H = 1.0$ TeV is used for the Born calculations, while $m_H = 10$ TeV is used for the K -matrix (KM) unitarized strong coupling case.

Process	$\eta_C = 1$	$\eta_C = 1.5$	$\eta_C = 2$
$W^+W^+ \rightarrow W^+W^+$	25 (12)	69 (34)	178 (89)
$W_L^+W_L^+ \rightarrow W_L^+W_L^+$	9 (4)	17 (7)	25 (11)
$W^+W^+ \rightarrow W_T^+W_T^+$	14 (8)	46 (24)	135 (71)
$W_L^+W_L^+ \rightarrow W_L^+W_L^+$ (KM)	17 (7)	31 (12)	43 (17)

ture functions and slightly different cuts, our $\eta_C = 1.5$ results in Table II are in excellent agreement with theirs. The differences in the $W_L^+W_L^+ \rightarrow W_L^+W_L^+$ cross sections are attributable to our use of nonleading terms in the longitudinal W distribution function.

III. UNITARITY EFFECTS

Given the large number of transversely polarized W^+ pairs produced in W^+W^+ scattering, it is important to understand how the contribution from longitudinally polarized like-charge pairs can be isolated if the method proposed in Ref. [5] for studying the electroweak symmetry breaking mechanism is to be realized. For $0.5 \text{ TeV} \leq m_H \leq 1 \text{ TeV}$, it has been shown that there are cuts which can enhance the longitudinal signal [7, 9]. However, as originally suggested by Chanowitz and Golden [5], it is possible that the Higgs sector is strongly interacting, in which case the effective- W approximation may be the only practical way to treat $W W$ scattering.

We explore this possibility by computing $W_L^+W_L^+$ elastic scattering for large m_H using several unitarized versions of the s -wave $I = 2$ weak isospin amplitude. The real and imaginary parts of this amplitude have been computed [16–18] to the one-loop level. In the limit $s \ll m_H^2$, the $I = 2$ amplitude takes the form

$$c_{I=2} = c_{I=2}^{(1)} + c_{I=2}^{(2)}, \quad (1)$$

$$c_{I=2}^{(1)} = -\frac{1}{2}fs, \quad (2)$$

$$c_{I=2}^{(2)} = \frac{f^2s^2}{2\pi} \left[-\frac{10}{9} \ln \left(\frac{s}{m_H^2} \right) - \frac{631}{108} + \sqrt{3}\pi + \frac{\pi}{2}i \right], \quad (3)$$

TABLE II. The results of the effective- W calculations performed in this paper are compared with the results of Ref. [7]. Both calculations impose a rapidity cut of 1.5 and the entries are the total cross sections in femtobarns.

Process	$m_{WW} \geq 0.8 \text{ TeV}$		$m_{WW} \geq 1 \text{ TeV}$		$m_{WW} \geq 1.2 \text{ TeV}$	
	Eff- W	Ref. [7]	Eff- W	Ref. [7]	Eff- W	Ref. [7]
$W_L^+W_L^+ \rightarrow W_L^+W_L^+$ (0.5 TeV)	3	3	1	1.5	.6	.8
$W_L^+W_L^+ \rightarrow W_L^+W_L^+$ (1 TeV)	10	11	6	7.1	3	4.5
$W^+W^+ \rightarrow W_T^+W_T^+$ (1 TeV)	22	19	11	11	5	6.9

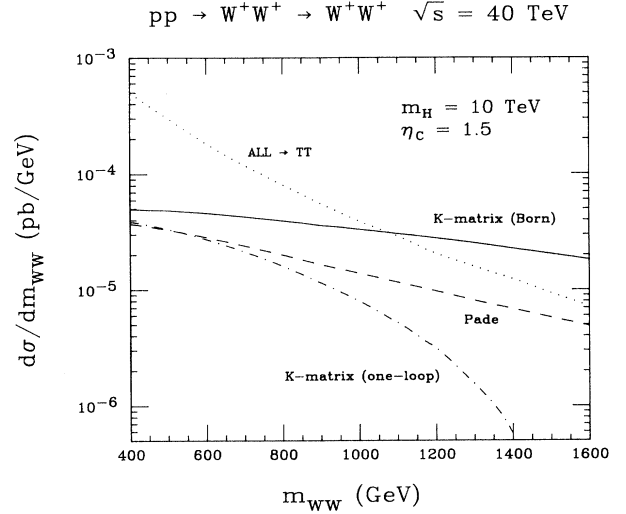


FIG. 5. The invariant-mass distributions resulting from unitarizing the s -wave W^+W^+ elastic amplitude are shown. The solid curve corresponds to the K -matrix unitarized Born term, the dot-dashed curve to the K -matrix unitarized Born plus one-loop amplitude, and the dashed curve to the [1,1] Padé unitarization. The dotted curve is the contribution of $W^+W^+ \rightarrow W_T^+W_T^+$.

with

$$f = \pi \frac{1}{(4\pi v_0)^2}, \quad v_0^2 = \frac{4m_W^2}{g^2}. \quad (4)$$

We use both the K -matrix [19, 20] and [1,1] Padé [21] unitarization schemes. In terms of the Born and one-loop s -wave projections $c_{I=2}^{(1)}$ and $c_{I=2}^{(2)}$, the corresponding unitarized amplitudes are

$$c_{I=2}^{\text{KM}} = \frac{c_{I=2}^{(1)} + \text{Rec}_{I=2}^{(2)}}{1 - i(c_{I=2}^{(1)} + \text{Rec}_{I=2}^{(2)})}, \quad (5)$$

$$c_{I=2}^{[1,1]} = \frac{c_{I=2}^{(1)2}}{c_{I=2}^{(1)} - c_{I=2}^{(2)}}. \quad (6)$$

The cross sections resulting from the unitarized amplitudes for $m_H = 10$ TeV are shown in Fig. 5. We have chosen $m_H = 10$ TeV because it is known that the [1,1] Padé unitarized weak isospin $I = 0$ s -wave amplitude has resonance of mass 1370 GeV for this value of the Higgs-boson mass [22, 23].

As can be seen from Fig. 5, K -matrix unitarization of the Born term for $m_H = 10$ TeV produces a significant increase in longitudinal pairs. This is quantified in the

TABLE III. Effective- W calculations of the total cross sections (in fb) for longitudinal and transverse W^+ pairs with (i) $m_{WW} \geq 0.8$ TeV; (ii) $m_{WW} \geq 1$ TeV; and (iii) $m_{WW} \geq 1.2$ TeV are given. A rapidity cut of 1.5 is imposed and $m_H = 10$ TeV is used.

Process	(i)	(ii)	(iii)
$W_L^+ W_L^+ \rightarrow W_L^+ W_L^+$ (KM)	22	15	9.1
$W_T^+ W_T^+ \rightarrow W_T^+ W_T^+$ (Born)	22	11	5.1

last line of Table I, which indicates that $\sigma(W_L^+ W_L^+)$ is almost doubled. Table III shows that the imposition of more restrictive m_{WW} cuts can suppress the $W^+ W^+ \rightarrow W_T^+ W_T^+$ background quite effectively.

Incorporation of the one-loop correction does not produce any additional enhancement. In fact, since $c_{I=2}^{(1)}$ and $\text{Rec}_{I=2}^{(2)}$ have opposite signs, the Padé unitarized amplitude yields a cross section which is approximately equal to that given by the Born term with $m_H = 1$ TeV (compare the dashed curves in Figs. 3 and 5). This difference in signs between $c_{I=2}^{(1)}$ and $\text{Rec}_{I=2}^{(2)}$ actually leads to a cancellation in the one-loop corrected K -matrix unitarized amplitude, which reduces the W_L^+ pair cross section below the Born term result.

IV. DISCUSSION AND CONCLUSIONS

The effective- W approximation is a simple tool for studying a variety of fusion processes. The agreement

between the approximate and the exact perturbative calculations has been shown to be excellent for the processes that involve an s -channel Higgs boson, especially in the vicinity of the Higgs-boson peak [24]. In the case of like-charge W pair production via the fusion mechanism, it is not at all clear that the exact and approximate calculations should agree because the transversely polarized pairs are dominant. However, for rapidity cuts $\eta_C \leq 2.0$, we find that the agreement is quite satisfactory.

Our inferences concerning a strongly interacting Higgs sector, obtained by using unitarized amplitudes and $m_H = 10$ TeV, are mixed. The K -matrix unitarized Born amplitude does predict a large increase in the number of longitudinally polarized W^\pm pairs. However, the unitarized one-loop corrections do not preserve this increase, and hence we cannot establish a plausible trend based on higher-order corrections and unitarization. The Born terms with $m_H = 1$ TeV are likely to give the most reliable estimate of the like-charge W pair cross section at energies reached at the Superconducting Super Collider.

ACKNOWLEDGMENTS

We wish to acknowledge useful conversations with Duane Dicus. One of us (A. A.) wishes to thank Department of Physics and Astronomy at Michigan State University for its hospitality. Computing resources were provided by Michigan State University and Ferris State University. This research was supported in part by the National Science Foundation under Grant No. 90-06117.

-
- [1] Particle Data Group, K. Hikasa *et al.*, Phys. Rev. D **45**, S1 (1992).
- [2] For a review of theoretical bounds on the Higgs-boson mass, see M. Sher, Phys. Rep. **179C**, 273 (1989).
- [3] J. F. Gunion, G. L. Kane, H. E. Haber, and S. Dawson, *The Higgs Hunter's Guide* (Addison-Wesley, Redwood City, CA, 1990).
- [4] M. S. Chanowitz and M. K. Gaillard, Nucl. Phys. **B261**, 379 (1985).
- [5] M. S. Chanowitz and M. Golden, Phys. Rev. Lett. **61**, 1053 (1988); **63**, 466(E) (1989).
- [6] D. A. Dicus and R. Vega, Phys. Lett. B **217**, 194 (1989).
- [7] V. Barger, K. Cheung, T. Han, and R. J. N. Phillips, Phys. Rev. D **42**, 3052 (1990).
- [8] R. Vega and D. A. Dicus, Nucl. Phys. **B329**, 533 (1990).
- [9] D. A. Dicus, J. F. Gunion, and R. Vega, Phys. Lett. B **258**, 475 (1991).
- [10] A. Abbasabadi and W. W. Repko, Phys. Rev. D **37**, 2668 (1988).
- [11] G. L. Kane, W. W. Repko, and W. B. Rolnick, Phys. Lett. **148B**, 367 (1984); S. Dawson, Nucl. Phys. **B249**, 42 (1985); J. Lindfors, Z. Phys. C **28**, 427 (1985).
- [12] For the Higgs width, we use the lowest-order contribution from the Higgs-boson decays into $W^+ W^-$, $Z^0 Z^0$, and $t\bar{t}$ ($m_t = 91$ GeV). For the lowest-order calculation, see L. Resnick, M. K. Sundaresan, and P. J. S. Watson, Phys. Rev. D **8**, 172 (1973); B. W. Lee, C. Quigg, and H. Thacker, *ibid.* **16**, 1519 (1977).
- [13] E. Eichten, I. Hinchliffe, K. Lane, and C. Quigg, Rev. Mod. Phys. **56**, 579 (1984); **58**, 1065(E) (1986).
- [14] A. Abbasabadi and W. W. Repko, Phys. Lett. B **199**, 286 (1987). For an exact perturbative calculation, see D. A. Dicus and R. Vega, Phys. Rev. Lett. **57**, 1110 (1986); J. F. Gunion, J. Kalinowski, and A. Tofighi-Niaki, *ibid.* **57**, 2351 (1986).
- [15] For the present work, we use the gauge-boson distribution functions that can be found in A. Abbasabadi and W. W. Repko, Phys. Rev. D **36**, 289 (1987); see also W. B. Rolnick, Nucl. Phys. **B274**, 171 (1986); P. W. Johnson, F. I. Olness, and W.-K. Tung, Phys. Rev. D **36**, 291 (1987); Z. Kunszt and D. E. Soper, Nucl. Phys. **B296**, 253 (1988).
- [16] S. Dawson and S. S. D. Willenbrock, Phys. Rev. Lett. **62**, 1232 (1989); Phys. Rev. D **40**, 2880 (1989).
- [17] M. Veltman and F. Yndurian, Nucl. Phys. **B325**, 1 (1989).
- [18] D. A. Dicus and W. W. Repko, Phys. Rev. D **42**, 3660 (1990).
- [19] W. W. Repko and C. J. Suchyta III, Phys. Rev. Lett. **62**, 859 (1989).
- [20] D. A. Dicus and W. W. Repko, Phys. Lett. B **228**, 503 (1989).
- [21] D. Bessis and M. Pusterla, Nuovo Cimento **LIV A**, 243 (1968).
- [22] A. Dobado, M. J. Herrero, and T. N. Truong, Phys. Lett. B **235**, 129 (1990); **235**, 134 (1990); A. Dobado, *ibid.* **237**, 457 (1990).
- [23] D. A. Dicus and W. W. Repko, Phys. Rev. D **44**, 3473 (1991).
- [24] A. Abbasabadi, W. W. Repko, D. A. Dicus, and R. Vega, Phys. Rev. D **38**, 2770 (1988).